

Aqueous-phase detection of antibiotics and nitroaromatic explosives by an alkali-resistant Zn-MOF directed by an ionic liquid

Jian-Hua Qin,^a Ya-Dan Huang,^{a,b} Ming-Yu Shi,^a Hua-Rui Wang,^{*a} Min-Le Han,^a Xiao-Gang Yang,^{*a} Fei-Fei Li,^b
and Lu-Fang Ma^{a,c}

^a*College of Chemistry and Chemical Engineering, and Henan Key Laboratory of Function-Oriented Porous Materials, Luoyang Normal University, Luoyang 471934, China, E-mail: yxg2233@126.com.*

^b*College of Chemistry and Chemical Engineering, Henan Polytechnic University, Jiaozuo, 454000, PR. China.*

^c*College of Chemistry and Molecular Engineering, Zhengzhou University, Zhengzhou, 450001, PR. China.*

Supporting Information

Fig. S1 Schematic representation of the 4,8-connected topology (CaF_2).

Fig. S2 PXRD patterns for simulated and experimental **1** sample soaked in aqueous solutions over the pH range from 2 to 6.

Fig. S3 Thermogravimetric curve of **1**.

Fig. S4 Normalized excitation and emission spectra of H_4ptptc in solid state at room temperature.

Fig. S5 Fluorescence spectra (a) and decay curve (b) of **1**.

Fig. S6 Phosphorescence spectra (a) and decay curve (b) of **1**.

Fig. S7 The emission spectra for **1** dispersed in different solvents at room temperature.

Fig. S8-S20 Details of detecting of antibiotics of **1** in the aqueous phase.

Fig. S21-S29 Details of detecting of nitroaromatic explosives of **1** in the aqueous phase.

Fig. S30 Spectral overlap between normalized absorption spectra of selected antibiotics and the normalized emission spectra of **1** in water.

Fig. S31 Spectral overlap between normalized absorption spectra of selected nitroaromatic explosives and the normalized emission spectra of **1** in water.

Table S1. Crystallographic data and experimental details for **1**.

Table S2. Selected bond lengths (\AA) and angles ($^\circ$) for **1**.

Table S3. Summary of quenching constants (K_{sv}) of **1** for sensing different analytes at room temperature.

Table S4. HOMO and LUMO energies calculated for the analytes used at B3LYP/6-31G** level.

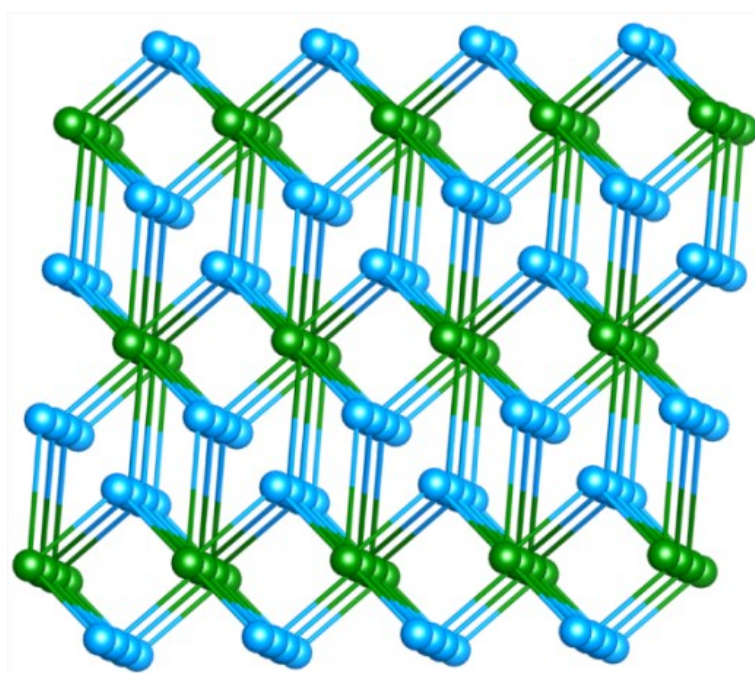
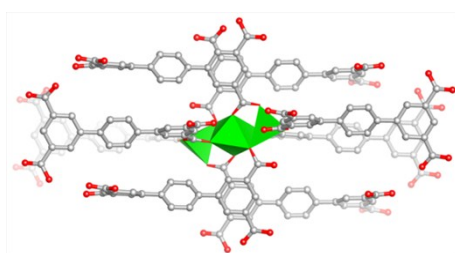
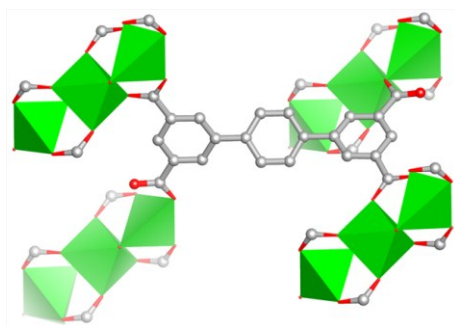


Fig. S1 Schematic representation of the 4,8-connected topology (CaF_2) (blue nodes for ptpc ligands and green nodes for $[\text{Zn}_3(\text{CO}_2)_8]$ clusters).

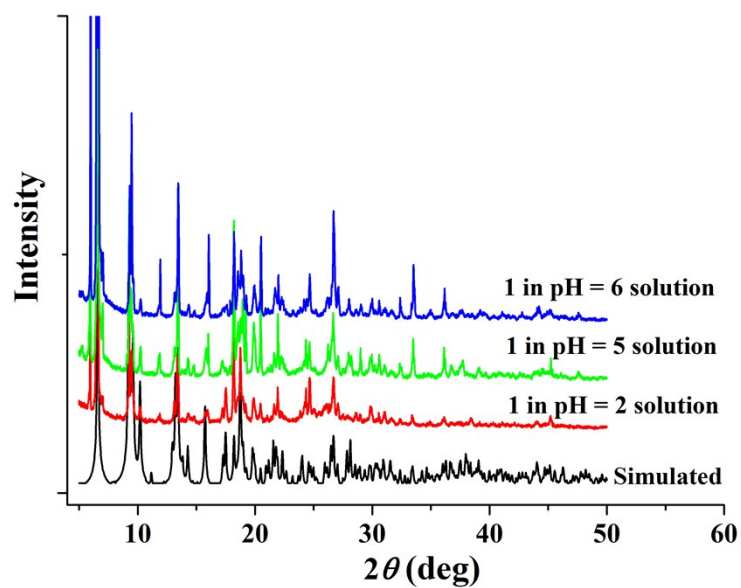


Fig. S2 PXRD patterns for simulated and experimental **1** sample soaked in aqueous solutions over the pH range from 2 to 6.

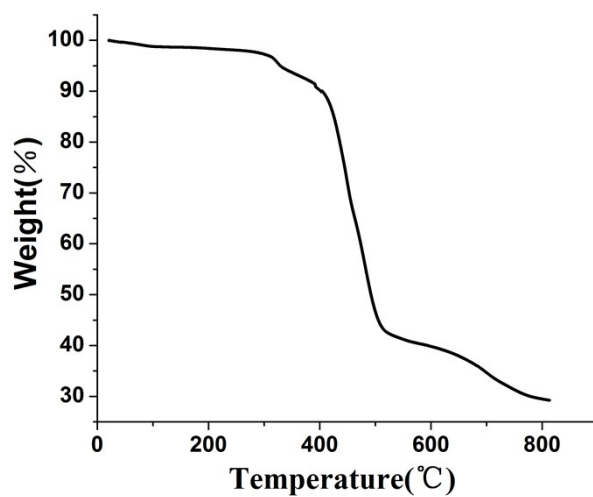


Fig. S3 Thermogravimetric curve of **1**.

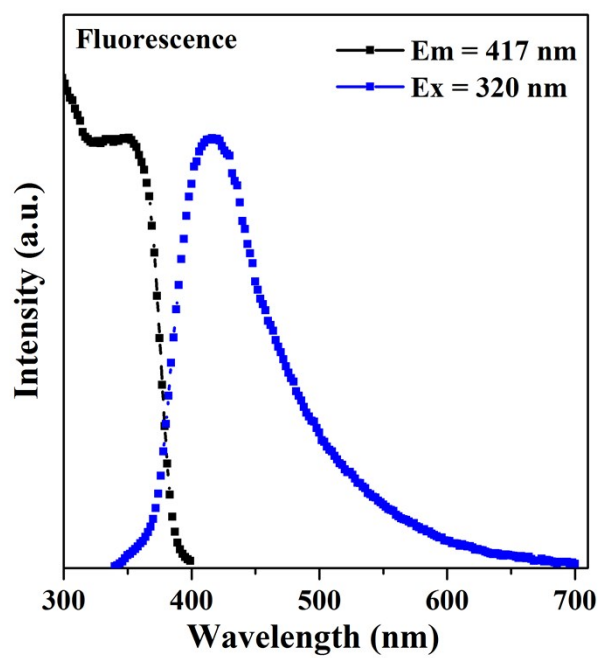
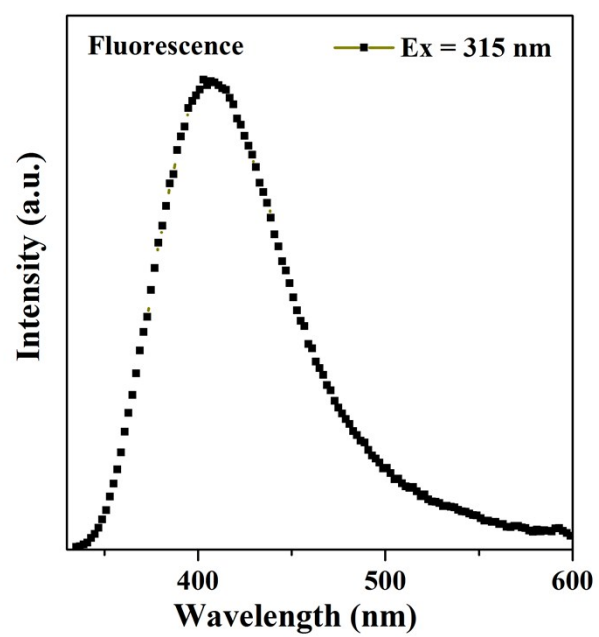
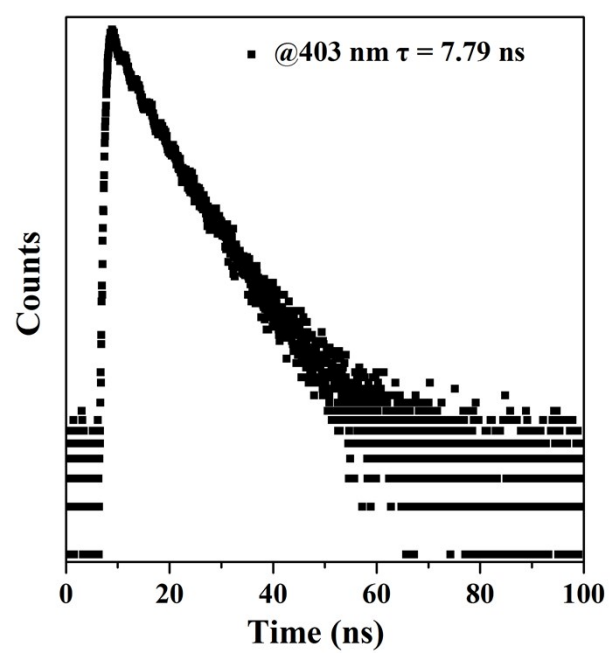


Fig. S4 Normalized excitation and emission spectra of H₄ptpc in solid state at room temperature.

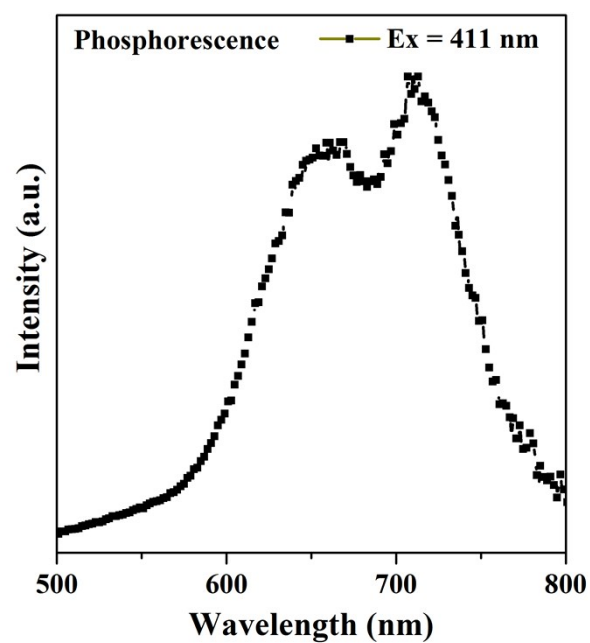


(a)

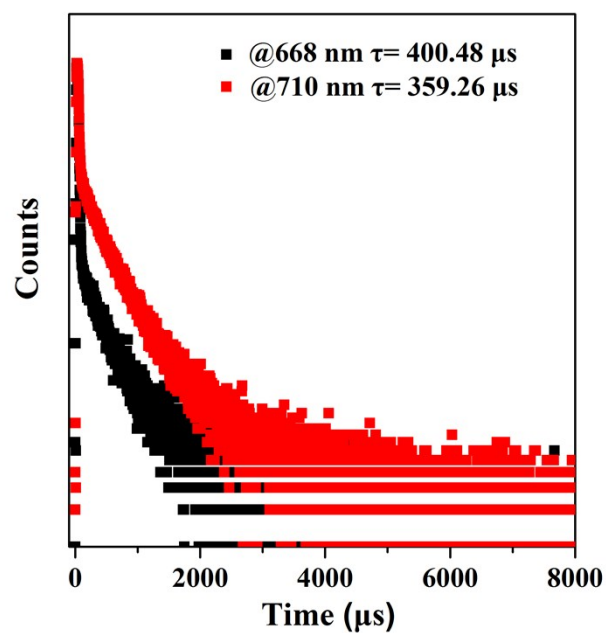


(b)

Fig. S5 Fluorescence spectra (a) and decay curve (b) of **1**.



(a)



(b)

Fig. S6 Phosphorescence spectra (a) and decay curve (b) of **1**.

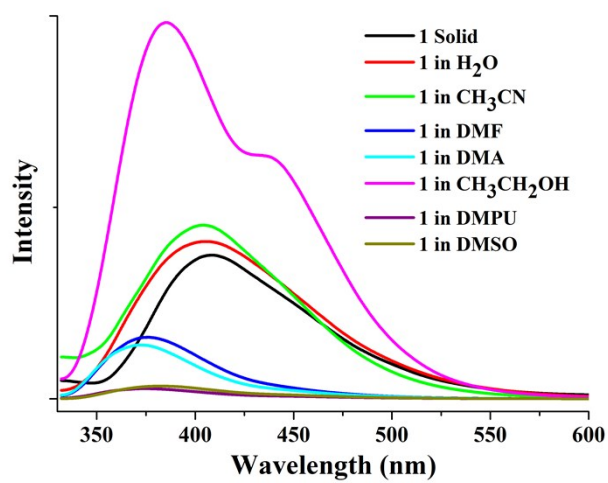


Fig. S7 The emission spectra for **1** dispersed in different solvents at room temperature.

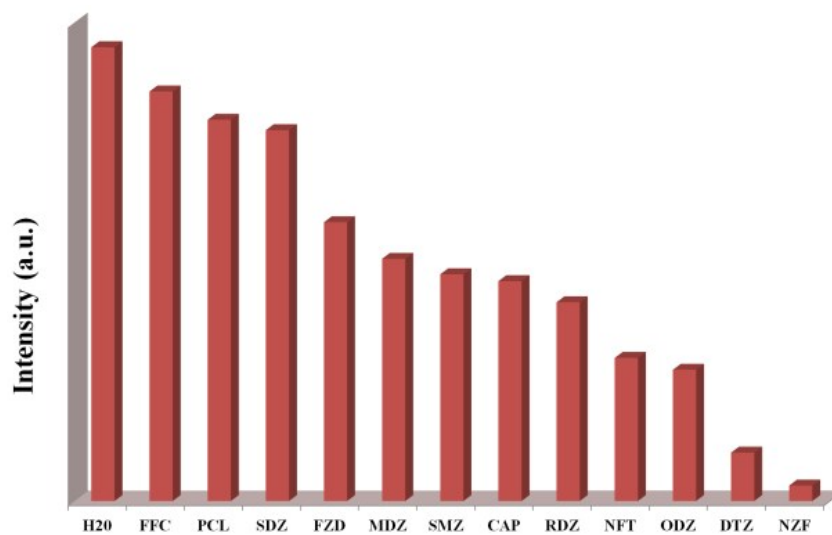


Fig. S8 The fluorescent intensity for **1** dispersed in 0.1 mM aqueous solutions of the selected antibiotics at room temperature.

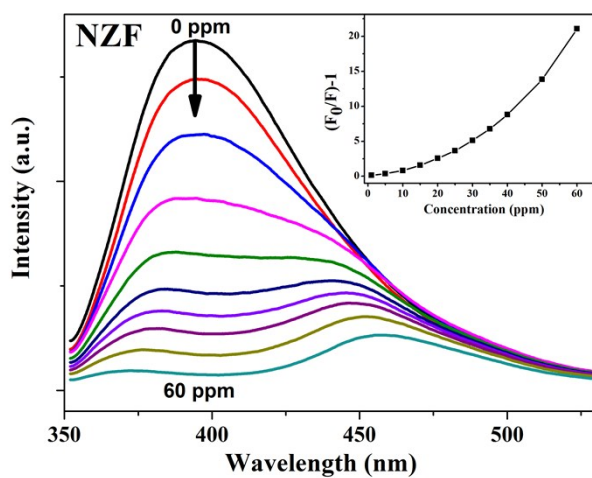


Fig. S9 Effect on the emission spectra of **1** dispersed in water upon incremental addition of NZF (inset: SV plots of NZF).

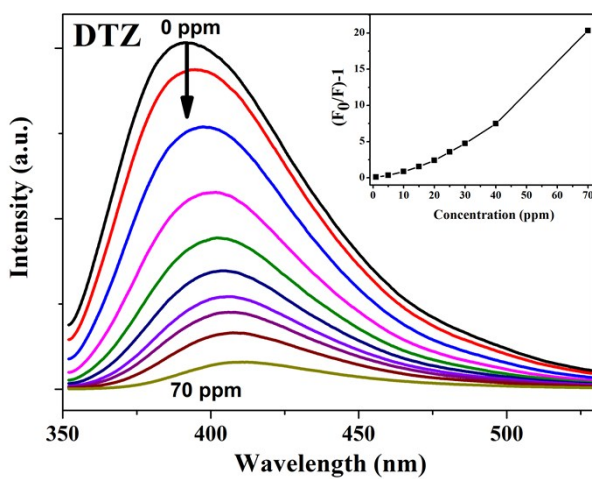


Fig. S10 Effect on the emission spectra of **1** dispersed in water upon incremental addition of DTZ (inset: SV plots of DTZ).

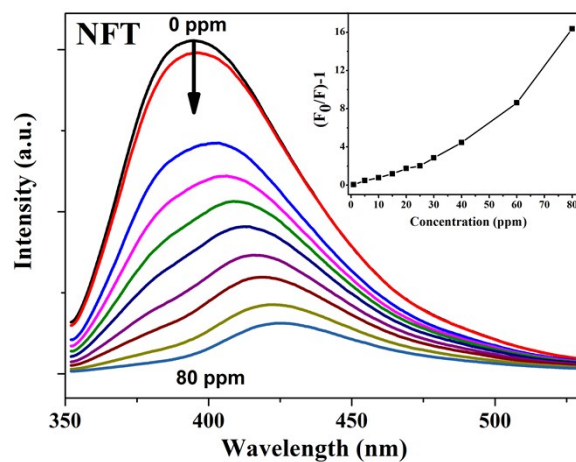


Fig. S11 Effect on the emission spectra of **1** dispersed in water upon incremental addition of NFT (inset: SV plots of NFT).

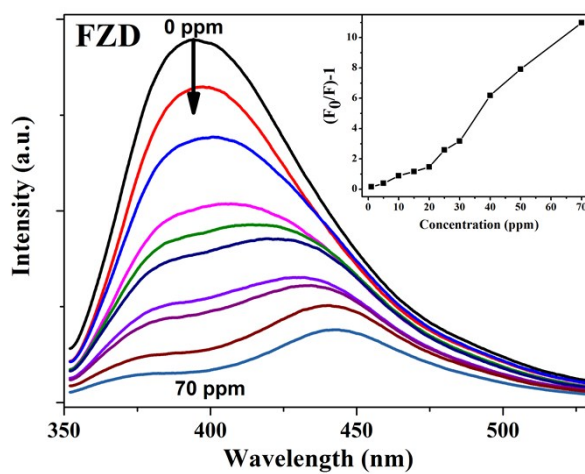


Fig. S12 Effect on the emission spectra of **1** dispersed in water upon incremental addition of FZD (inset: SV plots of FZD).

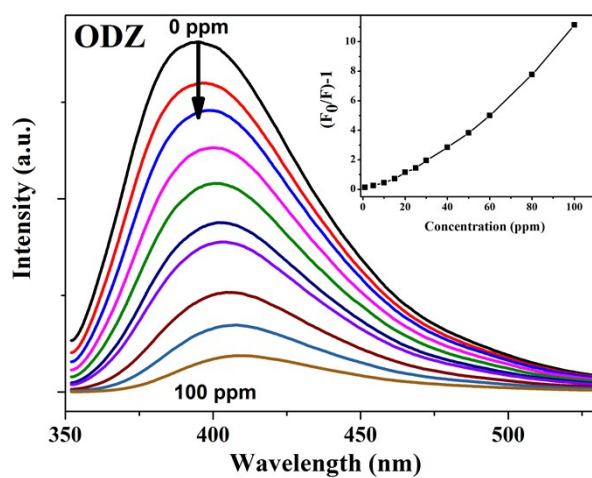


Fig. S13 Effect on the emission spectra of **1** dispersed in water upon incremental addition of ODZ (inset: SV plots of ODZ).

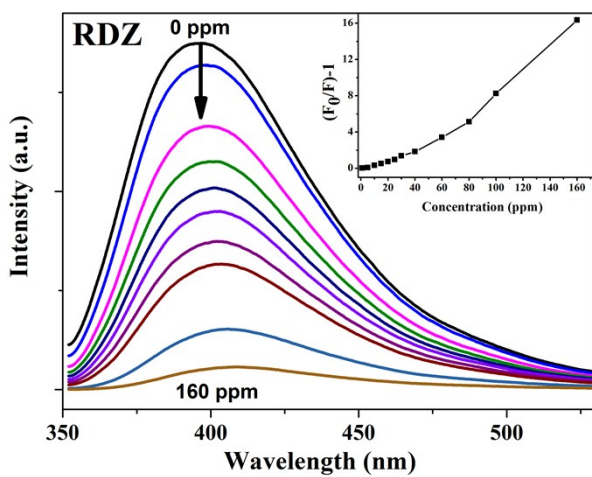


Fig. S14 Effect on the emission spectra of **1** dispersed in water upon incremental addition of RDZ (inset: SV plots of RDZ).

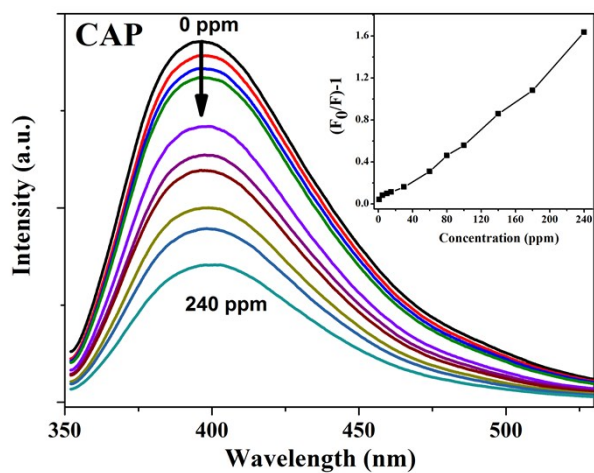


Fig. S15 Effect on the emission spectra of **1** dispersed in water upon incremental addition of CAP (inset: SV plots of CAP).

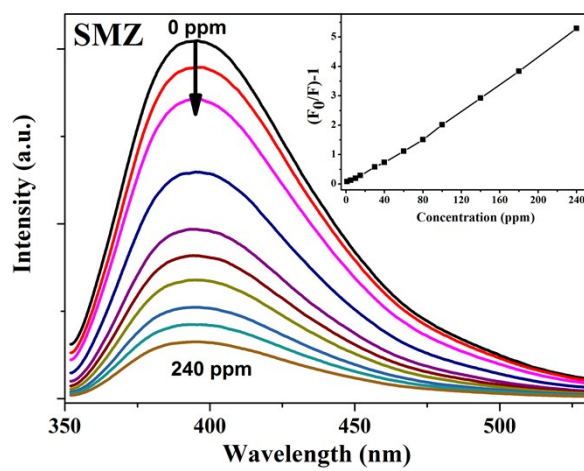


Fig. S16 Effect on the emission spectra of **1** dispersed in water upon incremental addition of SMZ (inset: SV plots of SMZ).

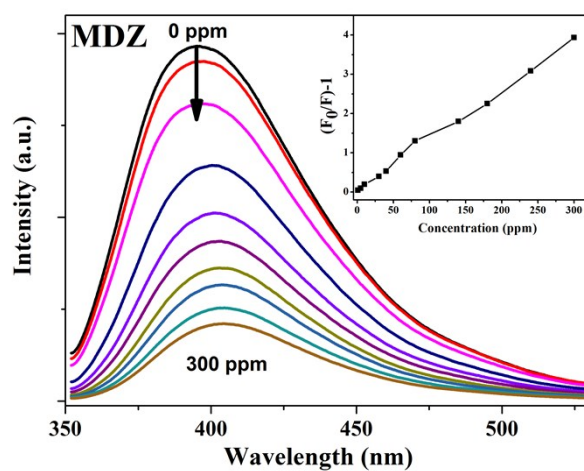


Fig. S17 Effect on the emission spectra of **1** dispersed in water upon incremental addition of MDZ (inset: SV plots of MDZ).

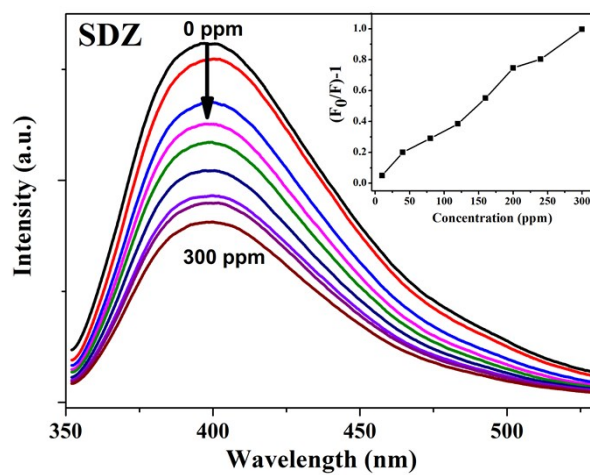


Fig. S18 Effect on the emission spectra of **1** dispersed in water upon incremental addition of SDZ (inset: SV plots of SDZ).

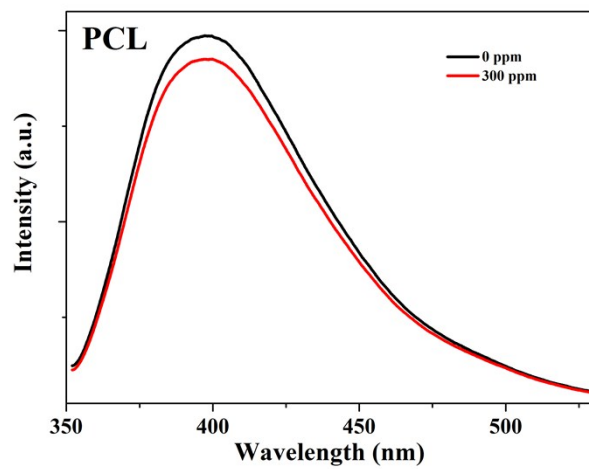


Fig. S19 Effect on the emission spectra of **1** dispersed in water upon incremental addition of PCL.

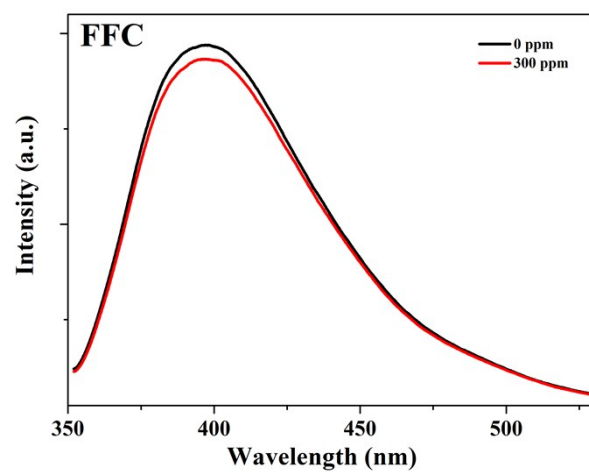


Fig. S20 Effect on the emission spectra of **1** dispersed in water upon incremental addition of FFC.

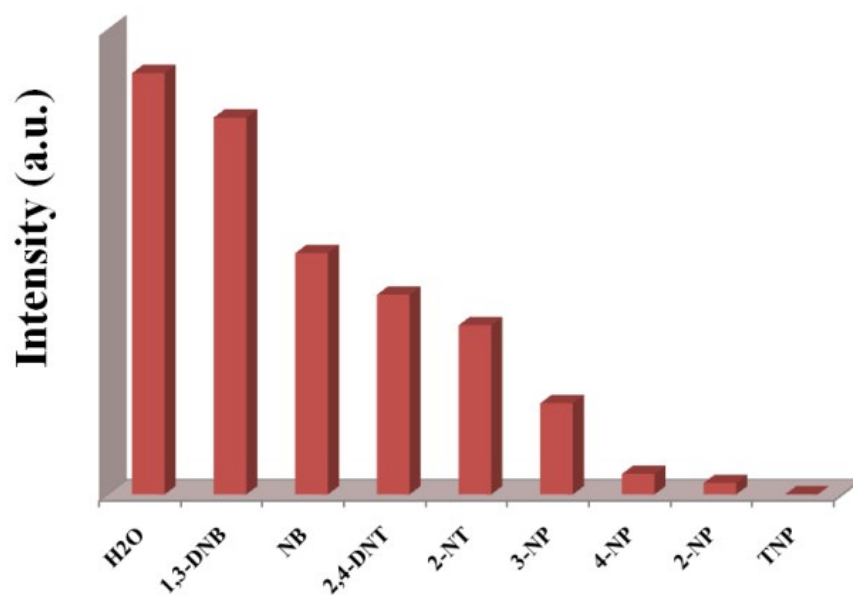


Fig. S21 The fluorescent intensity for **1** dispersed in 1 mM aqueous solutions of the selected nitroaromatic explosives at room temperature.

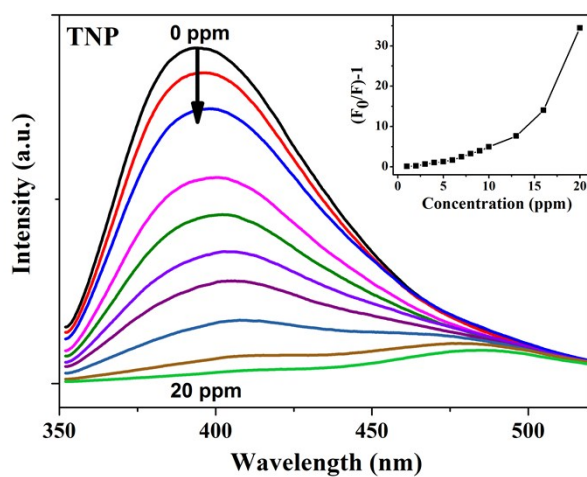


Fig. S22 Effect on the emission spectra of **1** dispersed in water upon incremental addition of TNP (inset: SV plots of TNP).

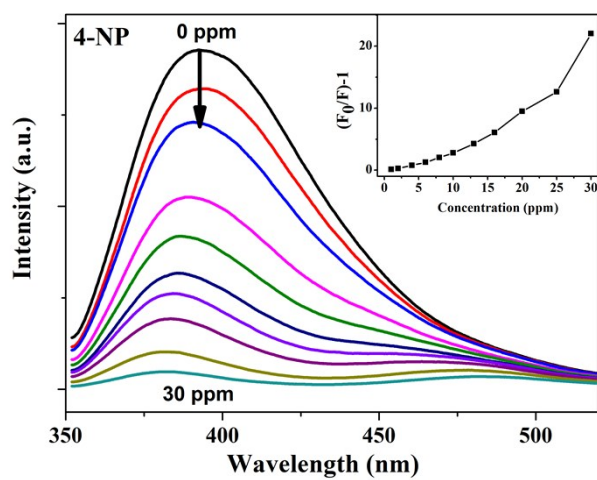


Fig. S23 Effect on the emission spectra of **1** dispersed in water upon incremental addition of 4-NP (inset: SV plots of 4-NP).

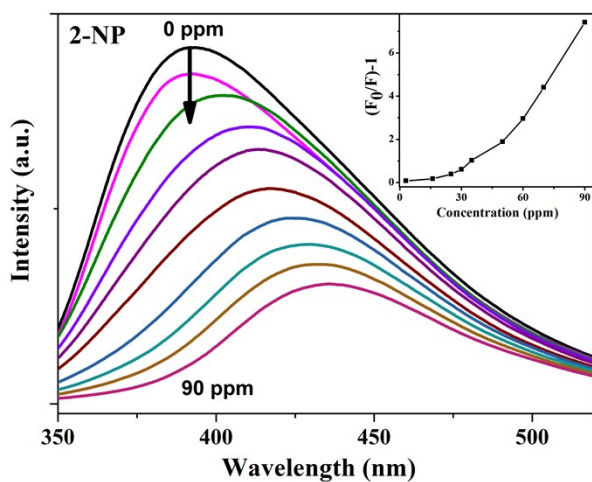


Fig. S24 Effect on the emission spectra of **1** dispersed in water upon incremental addition of 2-NP (inset: SV plots of 2-NP).

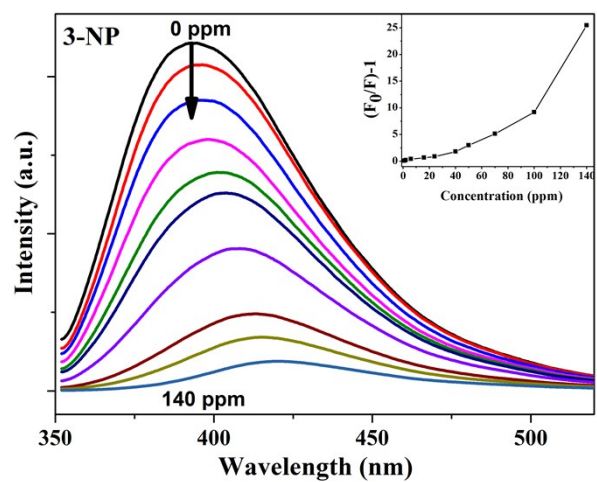


Fig. S25 Effect on the emission spectra of **1** dispersed in water upon incremental addition of 3-NP (inset: SV plots of 3-NP).

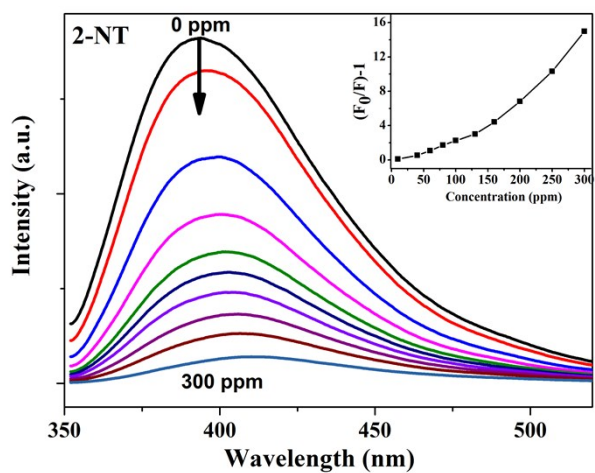


Fig. S26 Effect on the emission spectra of **1** dispersed in water upon incremental addition of 2-NT (inset: SV plots of 2-NT).

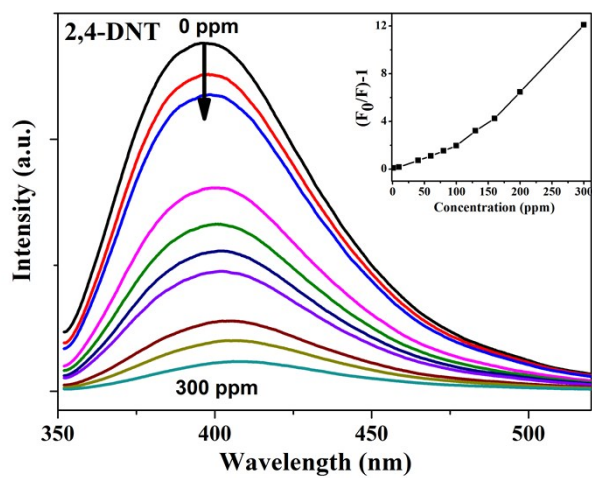


Fig. S27 Effect on the emission spectra of **1** dispersed in water upon incremental addition of 2,4-DNT (inset: SV plots of 2,4-DNT).

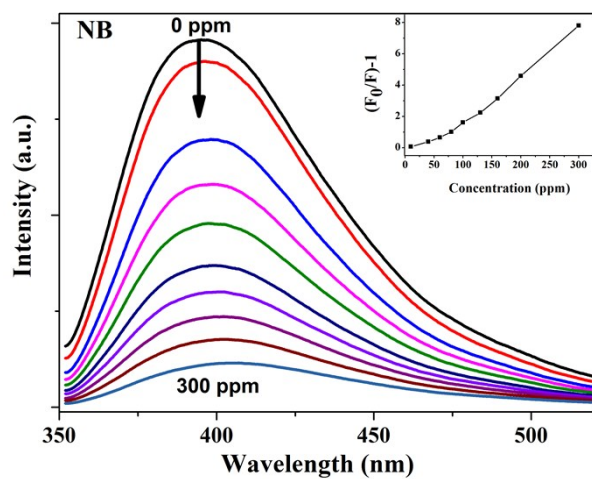


Fig. S28 Effect on the emission spectra of **1** dispersed in water upon incremental addition of NB (inset: SV plots of NB).

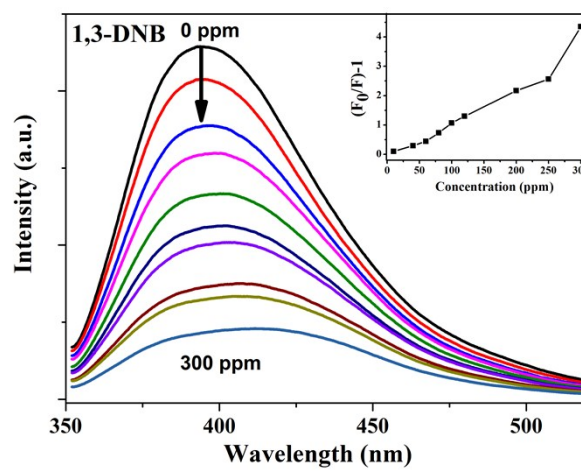


Fig. S29 Effect on the emission spectra of **1** dispersed in water upon incremental addition of 1,3-DNB (inset: SV plots of 1,3-DNB).

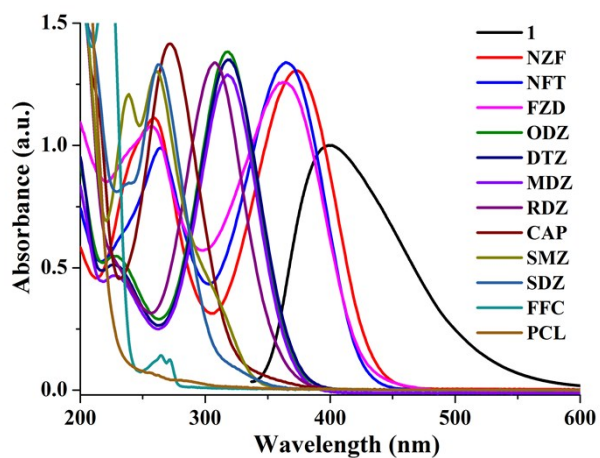


Fig. S30 Spectral overlap between normalized absorption spectra of selected antibiotics and the normalized emission spectra of **1** in water.

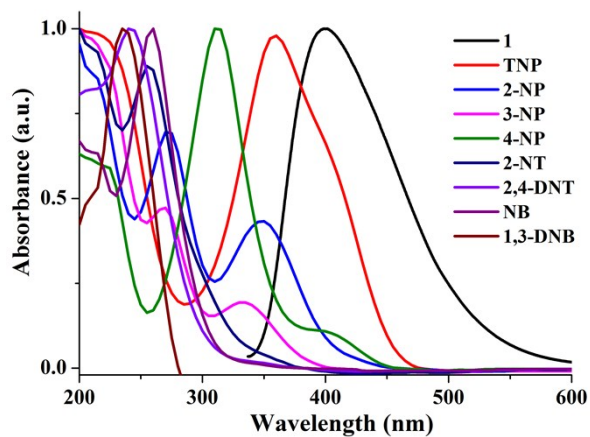


Fig. S31 Spectral overlap between normalized absorption spectra of selected nitroaromatics explosives and the normalized emission spectra of **1** in water.

Table S1. Crystallographic data and experimental details for **1**.

| Complex | 1 |
|---|--|
| Empirical formula | C ₆₀ H ₅₀ N ₄ O ₁₆ Zn ₃ |
| Formula weight | 1279 |
| Temperature/K | 293(2) |
| Crystal system | triclinic |
| Space group | P-1 |
| a/Å | 9.6166(4) |
| b/Å | 14.4465(6) |
| c/Å | 20.4967(10) |
| α/° | 106.767(4) |
| β/° | 98.427(4) |
| γ/° | 101.203(4) |
| Volume/Å ³ | 2611.6(2) |
| Z | 2 |
| ρ _{calc} /cm ³ | 1.273 |
| μ/mm ⁻¹ | 1.426 |
| F(000) | 1004.0 |
| Crystal size/mm ³ | 0.27 × 0.24 × 0.21 |
| Radiation | MoKα (λ = 0.71073) |
| 2θ range for data collection/° | 6.934 to 50.998 |
| Index ranges | -10 ≤ h ≤ 11, -17 ≤ k ≤ 17, -24 ≤ l ≤ 24 |
| Reflections collected | 19104 |
| Independent reflections | 9346 [R _{int} = 0.0352, R _{sigma} = 0.0565] |
| Data/restraints/parameters | 9346/0/604 |
| Goodness-of-fit on F ² | 1.042 |
| Final R indexes [I > 2σ (I)] | R ₁ = 0.0574, wR ₂ = 0.1442 |
| Final R indexes [all data] | R ₁ = 0.0690, wR ₂ = 0.1519 |
| Largest diff. peak/hole / e Å ⁻³ | 1.00/-2.07 |

$$R = \frac{\sum ||F_o| - |F_c||}{\sum |F_o|}, R_w = \sqrt{\frac{\sum w(|F_o|^2 - |F_c|^2)|^2}{\sum w(|F_o|^2)}}^{1/2}$$

Table S2. Selected bond lengths (Å) and angles (°) for **1**.

| Atom | Atom | Length/Å | Atom | Atom | Length/Å |
|------|------------------|----------|------|------------------|----------|
| Zn1 | O1 | 1.964(3) | Zn2 | O9 ⁵ | 2.021(3) |
| Zn1 | O4 ¹ | 2.183(3) | Zn2 | O12 ⁶ | 2.031(3) |
| Zn1 | O7 ² | 2.109(3) | Zn2 | O13 ⁷ | 1.986(3) |
| Zn1 | O10 | 1.977(3) | Zn3 | O2 ⁴ | 2.011(3) |
| Zn1 | O12 ³ | 2.271(3) | Zn3 | O4 ⁸ | 2.031(3) |
| Zn1 | O14 ⁴ | 2.095(3) | Zn3 | O8 | 2.000(3) |
| Zn2 | O5 | 1.976(3) | Zn3 | O16 ⁹ | 1.989(3) |

| Atom | Atom | Atom | Angle/° | Atom | Atom | Atom | Angle/° |
|------------------|------|------------------|------------|------------------|------|------------------|------------|
| O1 | Zn1 | O4 ¹ | 88.47(12) | O14 ⁴ | Zn1 | O12 ³ | 86.99(11) |
| O1 | Zn1 | O7 ² | 95.33(12) | O5 | Zn2 | O9 ⁵ | 101.70(13) |
| O1 | Zn1 | O10 | 177.12(13) | O5 | Zn2 | O12 ⁶ | 127.70(13) |
| O1 | Zn1 | O12 ³ | 91.47(12) | O5 | Zn2 | O13 ⁷ | 104.19(12) |
| O1 | Zn1 | O14 ⁴ | 84.29(12) | O9 ⁵ | Zn2 | O12 ⁶ | 111.85(12) |
| O4 ¹ | Zn1 | O12 ³ | 179.41(10) | O13 ⁷ | Zn2 | O9 ⁵ | 105.43(13) |
| O7 ² | Zn1 | O4 ¹ | 87.53(11) | O13 ⁷ | Zn2 | O12 ⁶ | 104.03(12) |
| O7 ² | Zn1 | O12 ³ | 91.90(10) | O2 ⁴ | Zn3 | O4 ⁸ | 110.90(11) |
| O10 | Zn1 | O4 ¹ | 94.20(12) | O8 | Zn3 | O2 ⁴ | 104.90(12) |
| O10 | Zn1 | O7 ² | 83.70(12) | O8 | Zn3 | O4 ⁸ | 102.96(12) |
| O10 | Zn1 | O12 ³ | 85.85(12) | O16 ⁹ | Zn3 | O2 ⁴ | 103.48(13) |
| O10 | Zn1 | O14 ⁴ | 96.62(12) | O16 ⁹ | Zn3 | O4 ⁸ | 128.67(13) |
| O14 ⁴ | Zn1 | O4 ¹ | 93.59(11) | O16 ⁹ | Zn3 | O8 | 103.62(12) |
| O14 ⁴ | Zn1 | O7 ² | 178.81(11) | | | | |

¹1+X,+Y,+Z; ²1+X,1+Y,+Z; ³-1+X,+Y,+Z; ⁴-1+X,-1+Y,+Z;

⁵-X,1-Y,-Z; ⁶1-X,1-Y,-Z; ⁷1-X,2-Y,-Z; ⁸+X,-1+Y,+Z; ⁹1-X,2-Y,1-Z.

Table S3. Summary of quenching constants (K_{sv}) of **1** for sensing different analytes at room temperature.

| Analytes | K_{sv} (ppm ⁻¹) | Analytes | K_{sv} (ppm ⁻¹) |
|----------|-------------------------------|----------|-------------------------------|
| NZF | 1.7×10^{-1} | TNP | 5.3×10^{-1} |
| DTZ | 1.6×10^{-1} | 4-NP | 3.8×10^{-1} |
| FZD | 1.0×10^{-1} | 2-NP | 1.9×10^{-2} |
| ODZ | 6.3×10^{-2} | 3-NP | 3.2×10^{-2} |
| NFT | 9.1×10^{-2} | 2-NT | 2.8×10^{-2} |
| RDZ | 4.6×10^{-2} | 2,4-DNT | 2.5×10^{-2} |
| CAP | 6.4×10^{-3} | NB | 2.1×10^{-2} |
| SMZ | 1.7×10^{-2} | 1,3-DNB | 1.1×10^{-2} |
| MDZ | 1.3×10^{-2} | | |
| SDZ | 3.3×10^{-3} | | |

Table S4. HOMO and LUMO energies calculated for the analytes used at B3LYP/6-31G** level.

| Analytes | HOMO (eV) | LUMO (eV) | Band gap |
|----------------------|-----------|-----------|----------|
| PCL ¹ | -5.558 | -1.777 | 3.781 |
| SMZ ² | -5.63 | -1.82 | 3.81 |
| SDZ ¹ | -5.538 | -2.26 | 3.278 |
| FFC ² | -6.62 | -2.56 | 4.06 |
| ODZ ² | -4.97 | -3.02 | 1.95 |
| DTZ ² | -6.37 | -3.27 | 3.1 |
| MDZ ² | -6.41 | -3.34 | 3.07 |
| CAP ² | -6.35 | -3.42 | 2.93 |
| RDZ ² | -6.57 | -3.52 | 3.05 |
| NZF ² | -5.99 | -3.72 | 2.27 |
| NFT ² | -6.21 | -3.94 | 2.27 |
| FZD ² | -6.37 | -4.06 | 2.31 |
| NB ² | -6.59 | -3.43 | 3.16 |
| 2-NT ² | -6.51 | -3.31 | 3.2 |
| 1,3-DNB ³ | -7.9855 | -3.4311 | 4.5544 |
| 2,4-DNT ³ | -7.7645 | -3.2174 | 4.5471 |
| 4-NP ² | -6.34 | -3.87 | 2.47 |
| 3-NP ² | -6.32 | -3.75 | 2.57 |
| 2-NP ² | -6.24 | -3.44 | 2.8 |
| TNP ² | -7.39 | -4.97 | 2.42 |

1. B. Wang, X. L. Lv, D. W. Feng, L. H. Xie, J. Zhang, M. Li, Y. B. Xie, J. R. Li and H. C. Zhou, *J. Am. Chem. Soc.*, 2016, **138**, 6204-6216.
2. H. R. Fu, L. B. Yan, N. T. Wu, L. F. Ma and S. Q. Zang, *J. Mater. Chem. A.*, 2018, **6**, 9183-9191.
3. S. S. Nagarkar, B. Joarder, A. K. Chaudhari, S. Mukherjee and S. K. Ghosh, *Angew. Chem. Int. Ed.*, 2013, **52**, 2881-2885.